Optical mode confinement in the Al/SiO₂ disk nanocavities with hyperbolic dispersion in the infrared spectral region

Carla Bacco
Priscilla Kelly
Lyuba Kuznetsova

Optical mode confinement in the Al/SiO₂ disk nanocavities with hyperbolic dispersion in the infrared spectral region

Carla Bacco, Priscilla Kelly, and Lyuba Kuznetsova*
San Diego State University, Department of Physics, 5500 Campanile Drive,
San Diego, California 92182-1233, United States

Abstract. This paper presents the results of a numerical study of the optical mode confinement in whispering gallery mode disk nanocavities with hyperbolic dispersion using nanolayered Al/SiO₂ hyperbolic metamaterial with different Al fill fractions. The fundamental properties of the optical modes and resonance frequencies for the disk nanocavities are studied using the numerical finite-element method. Numerical simulations show that light can be well confined in a disk nanocavity with a radius of up to an order of magnitude smaller than free-space resonant wavelength. This paper will also focus on how Purcell factor and quality factor of the disk nanocavities are affected by the fill fraction of the aluminum in the nanolayered metamaterial. Potential future applications for disk nanocavities with hyperbolic dispersion include silicon photonics optical communications networks, ultrafast LEDs, and biological nanoparticles sensing. © *2016 Society of Photo-Optical Instrumentation Engineers (SPIE)* [DOI: 10.1117/1.JNP.10 .046003]

1 Introduction

An optical whispering gallery mode (WGM) microdisk cavity is a structure that confines light to small volumes via resonant recirculation.[1] Optical microcavities offer a high confinement of the electromagnetic field in a small volume, with dimensions comparable to the wavelength of light, which provides a unique system for the enhancement of light–matter interactions on the nanoscale. Optical devices based on WGM microcavities, such as lasers, LEDs, and sensors, are already in use for a wide variety of applications.[1] Other photonic structures, such as photonic crystal cavities, can also enhance the light–matter interaction by orders of magnitude, enabling the device's optical properties to be controlled externally, both optically[2] and electrically.[3]

Optical metamaterials present a unique opportunity for light–mater interaction enhancement and attaining special electromagnetic properties that are not found in nature.[4] An intriguing class of metamaterials, which exhibit an optical topological transition (OTT) from a closed ellipsoid to opened hyperboloid dispersion, has been recently studied.[5–7] The iso-frequency surface (IFS) is enclosed by

$$\frac{\omega^2}{c^2} = \frac{k_x^2 + k_y^2}{\varepsilon_\perp} + \frac{k_z^2}{\varepsilon_\parallel},$$

(1)

where the "$\varepsilon_\parallel$" and "$\varepsilon_\perp$" are the dielectric permittivity in the direction parallel and perpendicular to the sample surface, ω is the frequency, c is the speed of light in a vacuum, and k_x, k_y, k_z are x, y, z components of the wavevector, respectively (Fig. 1). This dispersion is described by an open hyperboloid when $\varepsilon_\parallel$ or $\varepsilon_\perp < 0$. The point where the permittivity changes sign is known as

*Address all correspondence to: Lyuba Kuznetsova, E-mail: lkuznetsova@mail.sdsu.edu
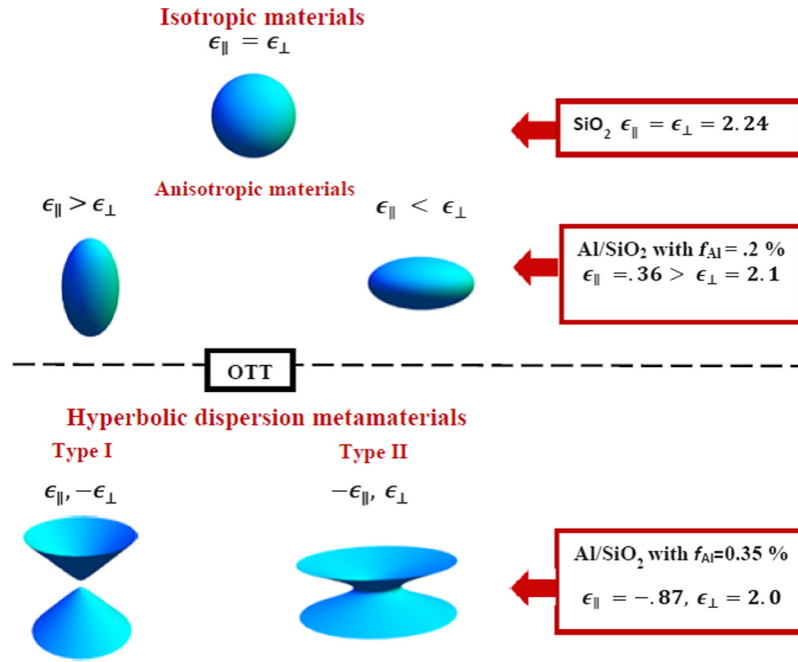
Fig. 1 A visualization of the changes in the isofrequency contour for the different types of dispersion. The values for the real part of the optical permittivity are given for a specific material (see Sec. 2).

an OTT.[5] The special property of propagating transverse-magnetic waves in such hyperbolic metamaterials (HMMs) is that the equation of a hyperboloid allows wavevectors with an unbounded magnitude. This is dramatically different from the spherical dispersion relation, which allows only wavevectors with the magnitude of $|k| = (\omega/c)$. Any waves with wavevectors larger than this cutoff will decay away exponentially in an isotropic medium. In contrast, propagating waves in a HMM have no wavevector cutoff in the effective medium limit. This important property of HMM allows dramatic increases of the photon density of states and much higher optical mode confinement.

In isotropic materials, e.g., silicon or SiO₂, reducing the size of the optical cavity (from microcavity to nanocavity) is limited to the fundamental diffraction limit.[8] In HMMs, large wavevectors can be achieved along the unbounded IFS. Therefore, optical WGM cavities, created from HMMs, allow the confinement of the electromagnetic field to an extremely small volume,[9,10] which opens new opportunities for creating infinitely small three-dimensional (3-D) nanocavities with hyperbolic dispersion and dimensions significantly smaller than the wavelength of light for applications in ultrafast LEDs.

In a microcavity, light is emitted into a cavity mode and acquires an enhanced efficiency or emission rate. The Purcell factor (F)[11] quantifies the enhancement of an atomic emission rate in a cavity versus its rate in free space

$$F = \frac{3Q(\lambda/n)^3}{4\pi^2 v_{\text{eff}}},\tag{2}$$

where Q is the cavity quality factor, λ is the resonant wavelength, n is the index of refraction of the cavity, and v_{eff} is the effective mode volume given by

$$v_{\text{eff}} = \frac{\int[\varepsilon(\vec{r})|\vec{E}(\vec{r})|^2]}{\max[\varepsilon(\vec{r})|\vec{E}(\vec{r})|^2]}.\tag{3}$$

Such enhancement is desired for both future quantum information processing and visible light communications. For example, a rate-equation model revealed that when a small (subwavelength) mode volume is combined with a Q (order of 100), the spontaneous emission rate for

an otherwise conventional LED can be enhanced, resulting in a 200-GHz modulation bandwidth.[12]

Here, we perform finite-difference element numerical simulations for the electromagnetic field confinement and study optical properties of the WGMs in such deep-subwavelength Al/SiO$_2$ disk nanocavities. This study aims to investigate the fundamental limits for the dimensions of this class of nanocavities, optical mode confinement, and the properties of the nanocavities' resonance frequencies. The choice of Al/SiO$_2$ HMMs nanolayered material and silicon substrate material will allow the future incorporation of such nanocavities to the well-established silicon photonics optical communications networks.[13]
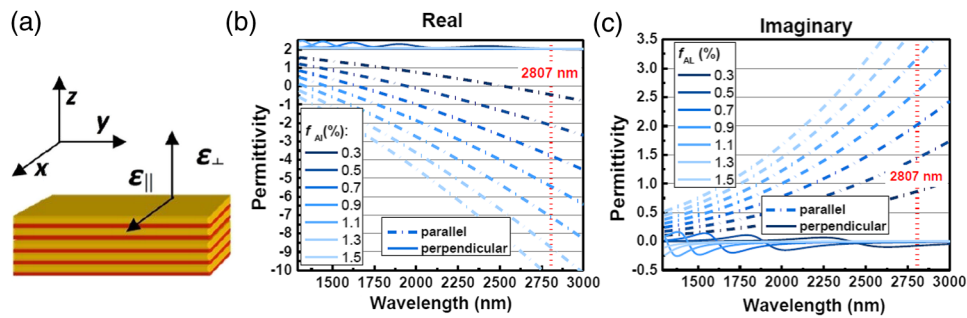
2 Nanolayered Metamaterial Permittivity Models

When designing 3-D nanocavities, the scale of each layer and dispersion of HMM is vital to increasing the bandwidth of such devices, which calls for a detailed model for the dispersion properties of multilayered HMMs. Using aluminum in metal-dielectric structures offers several advantages over these materials. In particular, the plasma frequency of the aluminum is higher than that of gold or silver, which allows for a significant surface plasmon response to occur in the ultraviolet (UV) portion of the spectrum. As a result, aluminum exhibits metallic characteristics over a broader spectral range than gold and silver. In addition, SiO$_2$ is used as the dielectric for this HMM because it could be easily integrated into current CMOS technology and has near-zero losses in the UV region.

In our recent work,[14] we used an effective medium approximation (EMA) with nonlocal corrections to describe Al/SiO$_2$ nanolayered structures with hyperbolic dispersion. Based on our previously published study (Ref. 14), we found that when the Al fill fraction is reduced to 1%, the number of layers does not affect the dielectric function of HMM (for $N > 25$). In addition, we found that the permittivity of the HMM does not change (Al fraction $\sim 0.3\%$) when the thickness of an individual layer is varied from 10 to 2 nm. For the simulations done in this paper, the disk nanocavity is assumed to be made of the Al/SiO$_2$ nanolayered HMM with 250 nm thickness. The number of the layers ($N = 25$) and the thickness of the individual layer ($d = 10$ nm) were constant. The Al/SiO$_2$ nanolayered structure is assumed to be a uniaxial material with different values for the dielectric permittivity in the parallel direction, $\varepsilon_\parallel$, and the perpendicular direction, $\varepsilon_\perp$. The permittivity is modeled using EMA.[15,16] According to EMA, in-plane permittivity, $\varepsilon_\parallel$, and out-of-plane permittivity, $\varepsilon_\perp$, can be described by

$$\varepsilon_\perp = \frac{(a_1 + a_2)\varepsilon_1\varepsilon_2}{a_2\varepsilon_1 + a_1\varepsilon_2},$$
$$\varepsilon_\parallel = \frac{a_1\varepsilon_1 + a_2\varepsilon_2}{a_1 + a_2}, \tag{4}$$

where a_1 is the thickness of aluminum layer (ε_1 optical permittivity) and a_2 is the thickness of SiO$_2$ layer (ε_2 optical permittivity). The EMA predicts the optical properties of a multilayered structure by combining the known permittivity of the two materials. The optical permittivity for aluminum was obtained by using Drude-critical points model while fitted experimental data from Ref. 17 was used in the infrared region. Silicon dioxide optical permittivity was modeled by using a polynomial fit for experimental data from Ref. 18, which is accurate for spectral range between 300 nm and 5 μm.

Manipulating the Al fill fraction (f_{AL}) controls the spectral position of the OTT. The optical permittivity predicted by EMA (Fig. 2) varies with wavelength and fill fraction, which allows for the designing of the material to fit the optical permittivity parameters in desired resonance range. The out-of-plane permittivity, $\varepsilon_\perp$, stays relatively constant while the in-plane permittivity, $\varepsilon_\parallel$, varies with small aluminum concentration. The optical permittivity values used for nanocavity studies are chosen near the OTT for a given frequency in an attempt to reduce the effects of the absorption.

Fig. 2 (a) Nanolayered HMM, (b) real and (c) imaginary parts of the out-of-plane optical permittivity (solid line), $\varepsilon_\perp$, and the in-plane optical permittivity (dashed line), $\varepsilon_\parallel$, for Al/SiO$_2$ metamaterials with aluminum fill fractions f_{AL} of 0.3% to 1.5%.
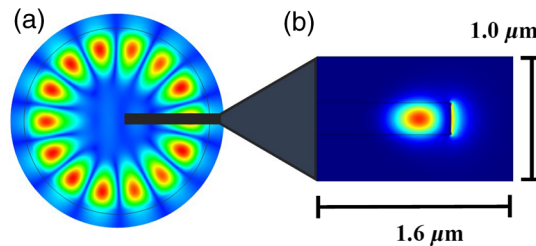
Fig. 3 (a) $m = 7$, radial electric intensity. (b) Diagram of computation space. The axisymmetric model displays one symmetric node of the resonance.

3 Computational Methods

COMSOL's multiphysics module was used to create a finite element method (FEM) study that produces a resonance frequency and optical mode intensity distribution for the disk nanocavities with different radii. FEM solves a set of weak partial differential Maxwell equations to find the relevant modes.[19] The optical mode volume and quality factor were deduced from the intensity distribution. The FEM model is axisymmetric, which is computationally efficient as it allows for symmetric modes to be extrapolated. Over a two-dimensional space, from the edge to the center of the disk, the electric field, electric displacement, and magnetic field were calculated as though they are mirrored around the disk in an azimuthal order (m) number of times (Fig. 3). Perfectly matched layers, which are not depicted here, were used to simulate infinite space beyond the computation space.

A free triangular mesh was used in the simulation. To ensure triangular mesh properties did not affect the solution, both a Delaunay mesh and a free quadrature mesh were implemented. Changing the mesh type had a minimal effect on the overall simulation (difference <0.1%). The smallest mesh settings offered by the COMSOL program are "extra fine" and "extremely fine." The respective maximum mesh size elements are 32.6 and 16.3 nm. The "extremely fine" mesh was used on disks with radii of 200 nm and lower. Finally, this proved to be adequate as the solutions converged with a tolerance of 1×10^{-6} and retained resolution.

While this model allows for exceptional computation times, the axisymmetric nature of this model does not always provide a clear picture of the modes. When reducing mode order to $m = 1$, higher order modes are hard to distinguish from the lowest order mode. FEM models also create spurious mode solutions that solve the required weak form partial differential equations, but have no physical counterpart. These factors must be taken into account for this numerical study.

4 Optical Mode Confinement: Results and Discussion

First, the SiO$_2$ microdisks with various radii (microdisk's height is 250 nm) were studied using the FEM model (Fig. 4). The free space wavelength λ_0 of the cavity in Fig. 4 (radius $R = 1$ μm)
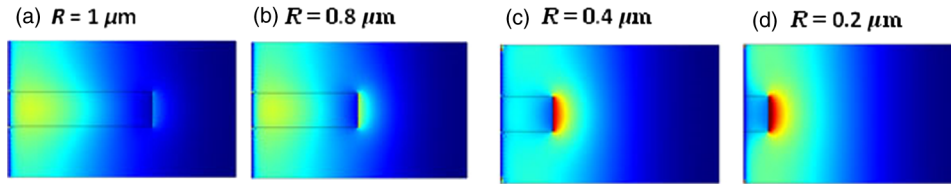
Fig. 4 $|E_{\text{rad}}|^2$ for the lowest order optical mode for the SiO$_2$ microdisks with different radii R. The resonance frequencies are (a) 105.98 THz ($R = 1\ \mu$m), (b) 107.14 THz ($R = 0.8\ \mu$m), (c) 109.72 THz ($R = 0.4\ \mu$m), and (d) 111.06 THz ($R = 0.2\ \mu$m).
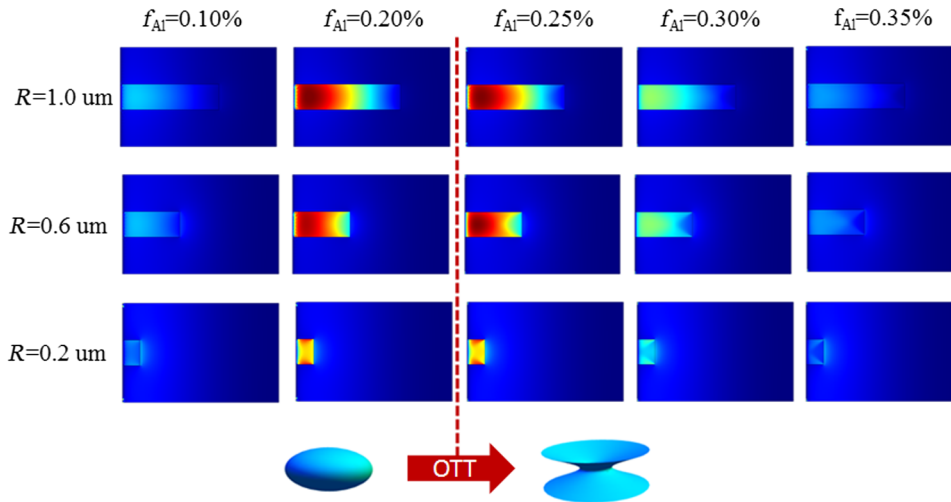

Fig. 5 $|E_{\text{rad}}|^2$ for the lowest order optical mode for disk nanocavities with different radii R and varying aluminum fill fractions f_{Al}. The optical constants were defined in Sec. 2.

is $\lambda_0 \sim 2828$ nm. As the radius decreases, the optical power is leaked around the circumference of the disk. As expected, by $R = 0.4\ \mu$m, the majority of the optical intensity is outside the cavity and the Q factor is significantly reduced indicating that the mode is no longer confined within the cavity. Based on the wavelength of the lowest order mode, the diffraction limit for this microdisk optical cavity is around $R_d \sim 0.9\ \mu$m. It indicates (Fig. 4) that no optical mode is likely in microdisks with dimensions smaller than R_d. This result is consistent with previously published experimental and numerical results for silicon microcavities.[8]

The results of the numerical FEM study for disk nanocavities with different radii R (disk nanocavity's height is 250 nm) show that with hyperbolic dispersion present in the nanolayered Al/SiO$_2$ material, the optical mode is highly confined in the disk considerably beyond the diffraction limit (Fig. 5). The EMA was used (see Sec. 2) to obtain the dielectric permittivity in the parallel direction, $\varepsilon_\parallel$, and in the perpendicular direction, $\varepsilon_\perp$ for nanodisks with a different aluminum fill fraction f_{Al}. The wavelength of the optical lower order mode for a disk nanocavity with radius $R = 1\ \mu$m and various aluminum fill fractions was around $\sim$2810 nm [Fig. 6(c)]. Figure 5 shows the intensity of the lowest order mode (Al fill fraction is varied between 0.1% and 3.35%) as the radius of the disk is decreased. For all radii, the highest confinement for the optical mode is achieved at the positive side of the OTT with a fill fraction of aluminum between 0.25% and 0.225%. Figure 5 shows that the optical mode is well confined in a disk nanocavity with a radius of up to an order of magnitude smaller than the free-space resonant wavelength λ_0. Our recent experimental study[20] shows the feasibility of fabrication of the Al/SiO$_2$ nanolayered films with a low aluminum fill fraction using the RF sputtering technique.

As expected, the Q-factor diminishes rapidly with decreasing the microdisk's dimensions [Fig. 6(a)]. In addition, as the fill fraction is increased and the dielectric permittivity in the parallel direction becomes $|\varepsilon_\parallel| > 0$, the Q-factor is reduced due to presence of higher optical losses for HMMs [Fig. 6(a)]. However, the Purcell factor exhibits a different type of behavior
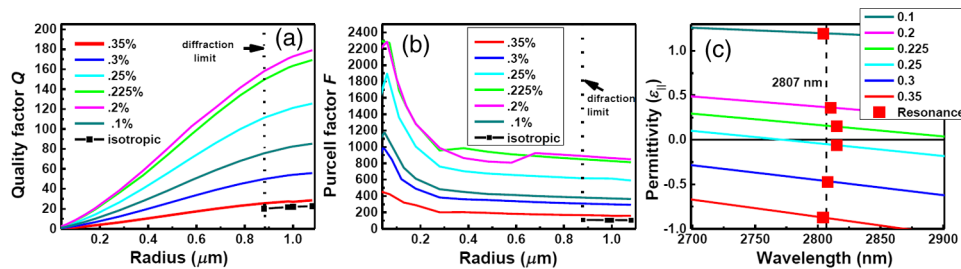
Fig. 6 (a) Quality factor Q and (b) Purcell factor F numerically calculated for the lowest optical mode of the disk nanocavities with different radii (between 60 nm and 1.08 μm) and aluminum fill fractions at wavelength $\lambda \approx 2800$ nm. The diffraction limit for SiO₂ nanocavity is indicated by a vertical dotted line ($R_d \sim 0.9$ μm). (c) Real part of the in-plane permittivity ($\varepsilon_\parallel$) and spectral position of the optical resonant wavelength for nanocavity with radius $R = 1$ μm and various aluminum fill fractions.

[Fig. 6(b)]. For the lowest order mode ($m = 1$), there is an increase in the Purcell factor for the disk nanocavity. It can be seen that the Purcell factor F is an order of magnitude higher for the disk HMM nanocavity compared to the isotropic case (SiO₂ microdisk) (Fig. 4). Further reducing the nanocavity size ($R < 60$ nm) leads to the drop in the F factor due to the reducing of the Q-factor ($Q < 10$) and, as a result, loss of the optical mode.

The disk nanocavity numerical study presented in this paper provides a valuable insight into the enhancement of the optical mode confinement due to hyperbolic dispersion. The strong optical mode confinement results in low radiation loss and, as a result, a higher Q factor for nanocavities from anisotropic nanolayered metamaterials compared to the nanocavities with isotropic dispersion. Circular disk geometry of a nanocavity results in a lower scattering loss for high-k wavevectors compared to the rectangular geometry studied in Ref. 21. The upper bound on the enhancement of the photonic density of states is imposed by the characteristic metamaterial patterning scale.[22] Using nanolayered metamaterial with the thickness of the individual layer approaching the atomic layer[23] could provide greater flexibility in designing disk nanocavities with highly confined optical modes. Possible incorporation of the laser gain material[24] will allow using this type of nanocavity for laser devices and ultrafast LEDs.

5 Conclusions

The numerical study of the Al/SiO₂ nanocavities with hyperbolic dispersion provides an opportunity to study the unique properties of nanocavities with increased photon density of states and enhanced light–matter interactions. Results of the numerical simulations show that nanocavities with radius of up to an order of magnitude smaller than λ_0 and Purcell factor reaching 2×10^3 are possible to create. Future incorporation of the laser gain material will allow using this type of nanocavity for laser devices and ultrafast LEDs for a variety of applications, from optical communications to biological nanoparticle sensing.

Acknowledgments

References

1. K. J. Vahala, "Optical microcavities," *Nature* **424**, 839–846 (2003).
2. Y. Zhang et al., "Photonic crystal nanobeam lasers," *Appl. Phys. Lett.* **97**, 051104 (2010).
3. B. Ellis et al., "Ultralow-threshold electrically pumped quantum dot photonic-crystal nanocavity laser," *Nat. Photonics* **5**, 297–300 (2011).

4. D. R. Smith, J. B. Pendry, and M. C. K. Wiltshire, "Metamaterials and negative refractive index," *Science* **305**(5685), 788–792 (2004).

5. H. N. S. Krishnamoorthy et al., "Topological transitions in metamaterials," *Science* **336**, 205–209 (2012).

6. M. Y. Shalaginov et al., "Broadband enhancement of spontaneous emission from nitrogen-vacancy centers in nanodiamonds by hyperbolic metamaterials," *Appl. Phys. Lett.* **102**, 173114 (2013).

7. D. Lu et al., "Enhancing spontaneous emission rates of molecules using nanopatterned multilayer hyperbolic metamaterials," *Nat. Nanotechnol.* **9**, 48–53 (2014).

8. J. Shainline et al., "Subwavelength silicon microcavities," *Opt. Express* **17**, 23323–23331 (2009).

9. X. Yang et al., "Experimental realization of three-dimensional indefinite cavities at the nanoscale with anomalous scaling laws," *Nat. Photonics* **6**, 450–454 (2012).

10. C. Bacco, P. Kelly, and L. Kuznetsova, "Optical mode confinement in three-dimensional Al/SiO$_2$ nano-cavities with hyperbolic dispersion," *Proc. SPIE* **9544**, 954419 (2015).

11. E. M. Purcell, "Spontaneous emission probabilities at radio frequencies," *Phys. Rev.* **69**, 37–38 (1946).

12. E. K. Lau et al., "Enhanced modulation bandwidth of nanocavity light emitting devices," *Opt. Express* **17**, 7790 (2009).

13. Y. Vlasov, "Applications of integrated photonics technology—from optical interconnects to neurophotonics," in *Advanced Photonics for Communications*, OSA Technical Digest (online) (Optical Society of America, 2014), paper JM1A.1 (2014).

14. P. Kelly, D. White, and L. Kuznetsova, "Theoretical design of nano-layered Al/SiO$_2$ metamaterial with hyperbolic dispersion with minimum losses," *Proc. SPIE* **9545**, 95450B (2015).

15. L. D. Landau, E. M. Lifshitz, and L. P. Pitaevskii, *Course of Theoretical Physics*, 2nd ed., Reed, Oxford (1984).

16. L. M. Brekhovskikh, *Waves in Layered Media*, 2nd ed., Academic, New York (1980).

17. A. Vial and T. Laroche, "Description of dispersion properties of metals by means of the critical points model and application to the study of resonant structures using the FDTD method," *J. Phys. D* **40**, 7152–7158 (2007).

18. R. Kitamura, L. Pilon, and M. Jonasz, "Optical constants of fused quartz from extreme ultraviolet to far infrared at near room temperatures," *Appl. Opt.* **46**, 8118–8133 (2007).

19. M. Oxborrow, "Traceable 2-D finite-element simulation of the whispering-gallery modes of axisymmetric electromagnetic resonators," IEEE Trans. Microwave Theory Tech. **55**, 1209–1218 (2007).

20. P. Kelly, A. Martin, and L. Kuznetsova, "Spectroscopic ellipsometry for anisotropic nano-layered Al/SiO$_2$ metamaterial with hyperbolic dispersion," *Proc. SPIE* **9919**, 991909 (2016).

21. J. Yao et al., "Three-dimensional nanometer-scale optical cavities of indefinite medium," *PNAS* **108**, 11327–11331 (2011).

22. Z. Jacob et al., "Engineering photonic density of states using metamaterials," *Appl. Phys. B* **100**, 215–218 (2010).

23. P. Kelly, M. Liu, and L. Kuznetsova, "Designing optical metamaterial with hyperbolic dispersion based on an Al:ZnO/ZnO nano-layered structure using the atomic layer deposition technique," *Appl. Opt.* **55**, 2993–2997 (2016).

24. J. Smalley et al., "Modal amplification in active waveguides with hyperbolic dispersion at telecommunication frequencies," *Opt. Express* **22**, 21088–21105 (2014).

Lyuba Kuznetsova is an assistant professor at the Physics Department at San Diego State University. She received her BS degree in physics from Moscow State University (Moscow, Russia), and her PhD in applied physics from Cornell University in 2008. She is the author of more than 30 journal papers and the coinventor on two patents. Her current research interests include nanophotonics, metamaterials, and lasers. She is a member of OSA and SPIE.

Biographies for the other authors are not available.